A Coupled Optoelectronic Oscillator With Performance Improved by Enhanced Spatial Hole Burning in an Erbium-Doped Fiber

Dan Zhu, *Member, IEEE*, Tianhua Du, and Shilong Pan, *Senior Member, IEEE*

***Abstract*—A coupled optoelectronic oscillator (COEO) with performance improved by the enhanced spatial hole burning (SHB) effect in an unpumped erbium-doped fiber (EDF) is proposed and demonstrated. In the proposed COEO, a strong standing-wave forming structure is incorporated to enable large SHB effect in the unpumped EDF, which significantly improves the supermode suppression ratio of the generated optical pulse, and the sidemode suppression ratio and phase noise performance of the generated electrical signal. A 10-GHz COEO is established. A stable optical pulse train is successfully generated with a supermode suppression ratio as high as 75 dB. The system is observed in the lab environment for 1.5 h with no significant variation. Without introducing any long fiber or multiloop structure in the optoelectronic oscillator loop, the sidemode suppression ratio of the 10-GHz RF output reaches 90 dB and the phase noise is about −130 dBc/Hz at 10-kHz offset. The influence of the optical power injected into the EDF, and the effects of the absorption coefficient and length of the EDF on the key parameters of the COEO are investigated and discussed.**

***Index Terms*—Coupled optoelectronic oscillator, fiber optics, microwave photonics, optical signal processing, unpumped erbium-doped fiber.**

I. Introduction

COUPLED optoelectronic oscillators (COEOs) have been widely studied in the past two decades for the capability of generating both optical pulses and RF signals with high quality [1]–[5], which are highly required in photonic microwave signal generation and processing in photonics-based radar, satellite payload applications and so on [6], [7]. The COEO is a combination of a mode-locked fiber laser and an optoelectronic oscillator (OEO) sharing an electro-optical modulator. The positive feedback between the OEO and the mode-locked fiber laser ensures the high quality of the generated optical pulses and RF signals [1]. For many applications, short optical pulses with a high repetition rate or low-phase-noise RF signals with a high frequency would be required, which demands the fiber laser mode-locked (or the OEO oscillated) at high-order harmonics of the cavity modes. As a result, the fiber laser cavity will support multiple oscillating modes spaced by the cavity's fundamental frequency. Considerable or even dominating noise associated with the generated optical pulses will be generated due to the beating among these supermodes. Thus for the optical pulse generation, one of the key performance indicators is the supermode suppression ratio. In order to improve the supermode suppression ratio, one effective way is to incorporate narrowband filters in the cavity, including comb filters [8] and composite cavities [9] and so on, but the wavelength drift would inevitably degrade the laser stability. Another way is to introduce inhomogeneous loss in the cavity [10] to reduce the pulse amplitude fluctuations, by using mechanisms of self-phase modulation followed by optical filtering [11], nonlinear polarization rotation effect [12], and optical pulse power feedback [13]. However, complex structures and precise alignments are usually needed. In addition, saturable absorbers including the semiconductor optical amplifier (SOA) [14], [15], the semiconductor saturable absorber mirror (SESAM) [16], [17] can be incorporated in the cavity to absorb the undesirable competitive modes. However, considerable noise would be introduced due to the carrier dynamics in the saturable absorbers and the output power would be limited because of the absorption [13].

On the other hand, sidemode suppression ratio and phase noise of the generated RF signal in the OEO loop are two other key performance indicators for COEOs [18], [19]. The sidemodes and the supermodes share the same origin in COEOs at the steady state. Many methods have been proposed to improve the sidemode suppression ratio [20]. For instance, a length of unpumped erbium-doped fiber (EDF) was incorporated in the laser cavity [21], in which the saturable absorption formed by the periodic spatial hole burning (SHB) [22] could largely suppress the sidemodes and evidently improve the stability of the oscillator. However, the standing waves in the EDF to excite the SHB effect are very weak, so the absorption of the undesirable sidemodes is usually limited. To overcome the problem, a dual-loop structure with two lengths of long fibers or a polarization-maintained dual-loop structure is inserted in the OEO loop to further suppress the sidemodes [21], [23], and the phase noise performance still needs improvement.

Manuscript received December 19, 2017; revised May 4, 2018 and June 12, 2018; accepted June 18, 2018. Date of publication June 21, 2018; date of current version July 12, 2018. This work was supported in part by the Natural Science Foundation of Jiangsu Province under Grant BK20160082, in part by the Jiangsu Provincial Program for High-level Talents in Six Areas under Grant DZXX-030, and in part by the Fundamental Research Funds for Central Universities under Grants NE2017002, NC2018005, and NS2016037. *(Corresponding author: Shilong Pan.)*

The authors are with the Key Laboratory of Radar Imaging and Microwave Photonics, Ministry of Education, Nanjing University of Aeronautics and Astronautics, Nanjing 210016, China (e-mail: danzhu@nuaa.edu.cn; thdu@nuaa.edu.cn; pans@nuaa.edu.cn).

Color versions of one or more of the figures in this paper are available online at http://ieeexplore.ieee.org.

Digital Object Identifier 10.1109/JLT.2018.2849561

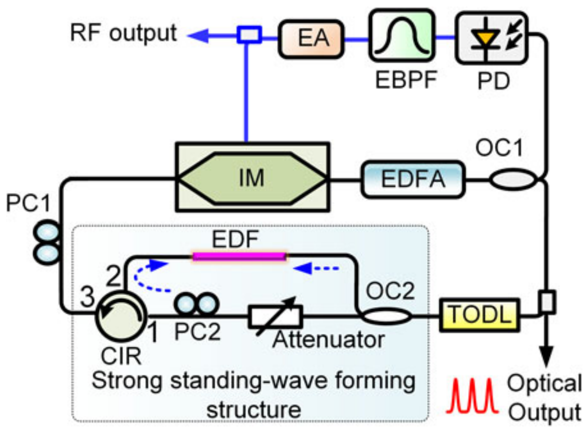

Fig. 1. The scheme of the proposed coupled optoelectronic oscillator (COEO) with a strong standing-wave forming structure using a length of unpumped EDF. PC: polarization controller; IM: intensity modulator; EDFA: erbium-doped fiber amplifier; EDF: erbium-doped fiber; OC: optical coupler; TODL: tunable optical delay-line PD: photodetector; EBPF: electrical bandpass filter; EA: electrical amplifier; CIR: optical circulator.

Recently, we have proposed a work using a novel structure to form strong standing waves in the unpumped EDF [24], which can greatly enhance the SHB effect to improve the system performance, including the supermode suppression ratio, the side-mode suppression ratio and the phase noise characteristics of the COEO. The strong standing wave is formed through a simple structure to guarantee the simplicity of the system, and the system performances in both optical and microwave domains are significantly improved without using long fiber or multi-loop structure. However, only some preliminary experimental results were reported, which is insufficient to understand the approach in-depth.

In this paper, a comprehensive theoretical and experimental investigation is performed on the COEO with performance improved by the enhanced SHB effect in an EDF. Section II introduces the principle of the proposed COEO. In Section III-A, a 10-GHz COEO is established and experimentally investigated. A 10-GHz stable optical pulse train is successfully generated with a supermode suppression ratio of 75 dB. The sidemode suppression ratio of the generated 10-GHz RF signal is as high as 90 dB, and the phase noise is about −130 dBc/Hz at 10-kHz offset. It should be noted that the above performance is achieved without introducing any long fiber or multi-loop structure in the OEO loop. In addition, Performance dependences of the optical power injected along the counter-propagating directions of the EDF, and the absorption coefficient and the length of the EDF are investigated and analyzed in Section III-B. In Section IV, conclusions and discussions are given.

II. Principle

The schematic diagram of the proposed COEO with performance improved by the enhanced SHB effect in an EDF is shown in Fig. 1, which consists of an OEO loop and a fiber laser loop sharing an intensity modulator (IM) followed by an optical coupler (OC1). An erbium-doped fiber amplifier (EDFA) is inserted to supply the optical gain. In the OEO loop, the output of OC1 is followed by a photodetector (PD), an electrical bandpass filter (EBPF), an electrical amplifier (EA), and then fed back to the RF port of the IM which is biased at the quadrature transmission point. For the mode-locked fiber laser loop, the other output of OC1 is followed by a tunable optical delay-line (TODL), a strong standing-wave forming structure incorporating an unpumped EDF, a polarization controller (PC) and the IM that is shared with the OEO loop. The TODL is used to tune the cavity length to match the two loops, PC1 is used to adjust the polarization state of the lightwave injected in the IM since the IM is polarization dependent, and the IM performs as the mode-locking device in the fiber laser loop.

The strong standing-wave forming structure is consisted of an OC (OC2), a length of unpumped EDF, and a 3-port optical circulator. The output of the TODL is split into two parts through OC2. Through the 3-port optical circulator, the two parts of lightwave are then injected into the unpumped EDF in counter-propagating directions, which form strong standing waves in the EDF. Since the optical components used are not polarization maintained, a second PC (PC2) is inserted in the lower branch to guarantee the consistency of the polarization states of the clockwise and counterclockwise injected optical signals in the EDF. Thus, enhanced SHB effect will be induced in the EDF, which results in weaker absorption for higher-power mode, and makes the undesirable competitive modes get smaller loop gain. In this way, the undesired supermodes will be suppressed.

The detailed explanation is as follows. The refractive index of the EDF changes spatially due to the SHB effect, resulting in periodical spatial variation of refraction index, given by the Kramers-Kronig relation [25]

$$\Delta n\left(z,\omega\right)=\frac{c}{\pi}P.V.\int_{\omega_1}^{\omega_2}\frac{\Delta\alpha\left(z,\omega'\right)}{(\omega')^2-\omega^2}d\omega' \tag{1}$$

where c is the light speed in vacuum, $P.V.$ is the principal value of the integral derived over the frequency range from ω_1 to ω_2, $\Delta\alpha$ is the variation of saturable absorption coefficient. From the standing wave theory, the spatial period is $\Lambda = \lambda/\, 2n_{\mathrm{eff}}$, where λ is the central wavelength and n_{eff} is the effective refraction index of the EDF. A weakly coupled fiber Bragg grating (FBG) is self-induced with a period of Λ, with the reflection response as follows [25]

$$R=\frac{\sin h^2\left(\sqrt{\kappa^2-\delta^2}L_g\right)}{\cos h^2\left(\sqrt{\kappa^2-\delta^2}L_g\right)-\delta^2/\kappa^2} \tag{2}$$

where $\delta = \beta\text{-}\pi/\lambda$ is the detuning, β is the mode propagation constant, $\kappa = 2\Delta n/(n_{\mathrm{eff}}\,\lambda)$ is the coupling coefficient of the FBG, Δn is the induced maximum refraction index change, L_{g} is the grating length. The corresponding full-width-half-maximum (FWHM) bandwidth is

$$\Delta f=\frac{c}{\lambda}\kappa\sqrt{\left(\frac{\Delta n}{2n_{eff}}\right)^2+\left(\frac{\Lambda}{L_g}\right)^2} \tag{3}$$

The filtering characteristic of the self-induced FBG affects the selection from the competitive modes in the mode-locked fiber laser cavity. Since the optical signal will circulate in the mode-locked fiber laser loop for many times, thus even very small cavity loss difference between the oscillating modes could be accumulated to form large output power difference. Thus the strong standing wave forming structure will improve the performance of the supermode suppression ratio of the generated optical pulses.

The strength of the forming standing wave is affected by the injected optical power values in the counter-propagating directions of the EDF, which will affect the formed SHB effect and further affect the suppression of the undesired modes. In addition, from Eq. (3), it can be seen that the filtering performance of the self-induced FBG is related to the induced refraction index change Δn and the length of the EDF. The induced refraction index change Δn is proportional to the doping concentration of Er^{3+} of the EDF [26]. Thus, the property of supermode suppression ratio is related with the injected optical power values in the counter-propagating directions of the EDF, the doping concentration and the length of the EDF. As compared with [9], the new structure could strongly enhance the SHB effect in the unpumped EDF and improve the performance of the COEO.

III. Experimental Results and Analyses

An experiment is carried out with the setup shown in Fig. 1. The IM (Fujitsu FTM7938EZ) has a 3-dB working bandwidth of 40 GHz; the PD (Conquer PIN-TIA) has a 3-dB working bandwidth of 10 GHz and a responsivity of 0.88 A/W; the EA is a low-noise one, which has a working frequency range of 8-18 GHz and a gain of 40 dB; the EBPF has a center frequency of 10.664 GHz and a 3-dB bandwidth of 11.8 MHz. An RF divider is inserted after the EA to tap out part of the generated RF signal in the OEO loop to measure the sidemode suppression ratio. The EDFs are produced by the Yangtze Optical Fibre & Cable Co. Ltd and have an absorption coefficient of 7, 13 and 22 dB/m @ 1530 nm, respectively. The EDFA (Amonics AEDFA-PA-35-B-FA) has a small signal gain of 30 dB. OC1 has a power splitting ratio of 9:1, with the 90% port connected to the fiber laser loop. OC2 has a power splitting ratio of 9:1, with the 90% power directly injected into the EDF. An optical power attenuator is inserted in the lower branch of the strong standing-wave forming structure to adjust the clockwise optical power injected into the EDF. An optical spectrum analyzer (AQ6370C, 0.02-nm resolution) is used to observe the optical spectra, and a digital sampling oscilloscope (DSO, Agilent 86100C with module 86116C) is engaged to observe the waveform of the output optical pulses. A signal source analyzer (Rohde & Schwarz FSWP, 1 MHz-50 GHz) is used to measure the electrical spectra and the phase noise performances.

A. COEO Incorporating the Unpumped-EDF Based Strong Standing-Wave Forming Structure

The optical pulse and RF signal generation with high quality based on the COEO incorporating the unpumped-EDF-based strong standing-wave forming structure is verified. A 1-m unpumped EDF with absorption coefficients of 13 dB/m @ 1530 nm is incorporated in the strong standing-wave forming structure shown in Fig. 1. Since the doping concentration characteristics of the EDFs are not supplied by the producer, thus the characteristic of the absorption coefficient of the EDF is used to represent the doping concentration level in this work [27]. Here the larger absorption coefficient represents larger doping concentration [28]. The output power of the EDFA is set to be about 17 dBm. The two optical signals from the two outputs of OC2 are injected into the EDF in counter-propagating directions. In order to research the influence of the formed standing wave with the system performance, the optical power in the clockwise direction is adjusted by tuning the inserted optical power attenuator while the power in the counterclockwise direction is kept 15.6 dBm. When the COEO reaches the stable oscillation state, the optical power injected into the PD in the OEO loop is about −1.6 dBm, and the modulated RF power at the IM is about 10 dBm. Fig. 2 shows the supermode suppression ratio versus the injected clockwise optical power in the unpumped-EDF based strong standing-wave forming structure. The supermode suppression performance is obtained from the electrical spectrum by directing the optical pulses into a PD (Conquer PIN-TIA), which also has a 3-dB working bandwidth of 10 GHz and a responsivity of 0.88 A/W. The injected optical power is about −2 dBm, and the measured RF power is about −3 dBm. As can be seen, with the injected clockwise optical power increased from about 0.2 dBm, the supermode suppression ratio increases from about 74.0 dB. When the clockwise optical power is tuned to be 2 dBm, the supermode suppression ratio reaches its maximal value of 75.2 dB. Then the supermode suppression ratio changes to be 74.1 dB when the clockwise optical power increases to 4 dBm. An optimum value of the clockwise optical power exists. For the results left from the optimum point, by increasing the clockwise optical power, the induced SHB effect is enhanced to improve the supermode suppression performance. Meanwhile, for the results right from the optimum point, the absorption effect will be too large with the increasing of the clockwise optical power, and the optical power in the mode-locked fiber laser loop will be greatly decreased. Thus the system performance will be deteriorated when the injected clockwise optical power is larger than the optimized one.

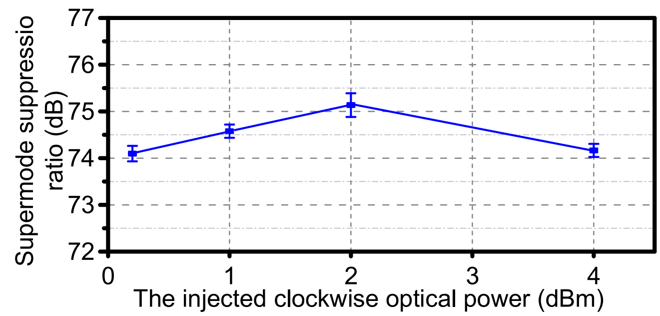

Fig. 2. Supermode suppression ratio versus the injected clockwise optical power when a 1-m unpumped EDF with an absorption coefficient of 13 dB/m @ 1530 nm is incorporated, and the optical power along the counterclockwise direction is 15.6 dBm.

The sidemode suppression ratio of the generated RF signal in the OEO loop versus the clockwise optical power is also investigated, as shown in Fig. 3, where the measured RF power

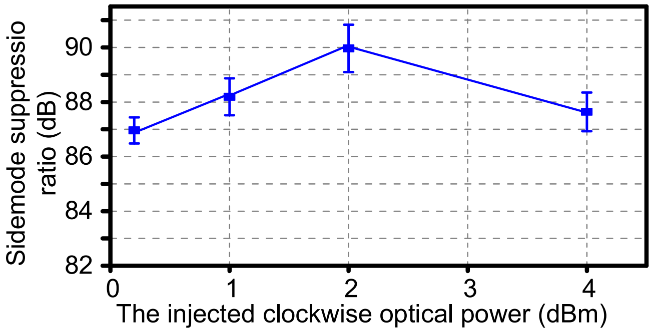

Fig. 3. Sidemode suppression ratio versus the injected clockwise optical power when a 1-m unpumped EDF with an absorption coefficient of 13 dB/m @ 1530 nm is incorporated, and the optical power in the counterclockwise direction is 15.6 dBm.

is about −3 dBm. As can be seen, with the injected clockwise optical power increased from about 0.2 to 2 dBm, the sidemode suppression increases from 87.0 dB to the optimized value of 90.0 dB. Then when the clockwise optical power is increased to 4 dBm, the supermode suppression ratio decreases to 87.6 dB. An optimum value of the clockwise optical power also exists for the sidemode suppression ratio performance. The phase noise performances of the generated RF signals from the COEO are also measured with the clockwise optical power tuned. The phase noise value @ 10 kHz offset is kept around -130 dBc/Hz with the injected clockwise optical power increased from 0.2 to 4 dBm. It means that in the condition of using the 1-m unpumped EDF with an absorption coefficient of 13 dB/m @ 1530 nm, the changing of the formed standing wave has limited impact with the phase noise performance of the generated RF signal in the OEO loop.

When the power in the counterclockwise and the clockwise direction is set to be 15.6 and 2 dBm, respectively, the eye diagram and the corresponding optical spectrum of the generated optical pulse is shown in Fig. 4(a) and (b), respectively. By injecting the generated optical pulse into a PD, the obtained electrical spectrum is shown in Fig. 4(c), from which it can be seen that the supermode suppression ratio is 75.4 dB. The electrical spectrum and the phase noise of the generated RF signal in the OEO loop are shown in Fig. 5(a) and (b), respectively. It can be seen that the sidemode suppression ratio of the generated microwave signal is 90.7 dB. The phase noise of the generated microwave signal is about −130.5 dBc/Hz at 10-kHz offset. In our experiment, the phase noise is measured using a signal source analyzer (Rohde & Schwarz FSWP, 1 MHz-50 GHz), for which the phase noise and the amplitude noise can be obtained separately. Thus the measured phase noise curve here has the amplitude noise cancelled. The timing jitter is calculated to be 128.9 fs (from 100 Hz to 10 MHz) for the SSB phase noise shown in Fig. 5(b). In our experiment, the fiber laser cavity has a length of about 36 m (except for the inserted EDF), giving a mode spacing of about 5 MHz in the fiber laser loop; and the OEO cavity has a length of about 16 m. The relatively short cavity lengths lead to a relatively larger mode spacing, which contributes to the performance improvement of the supermode suppression ratio in the fiber laser loop and the sidemode

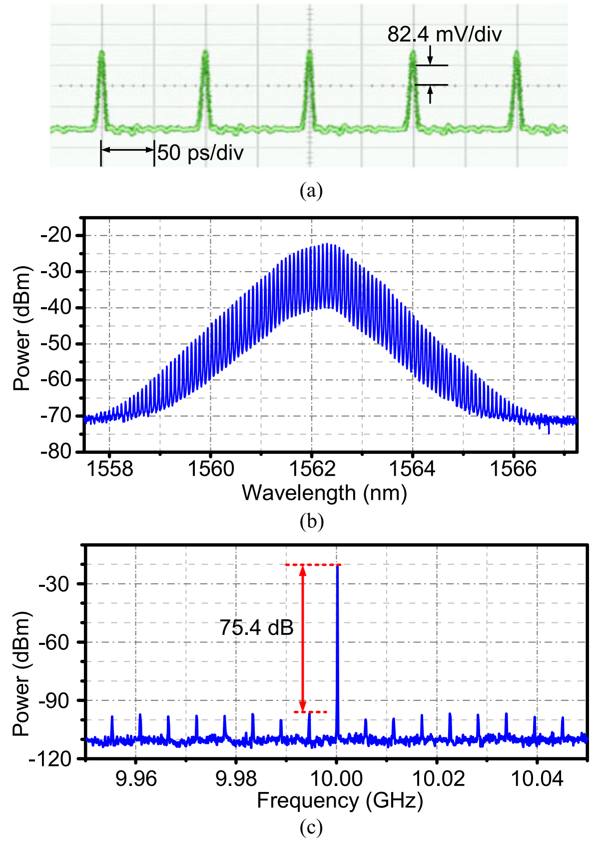

Fig. 4. (a) The waveform, (b) the optical spectrum and (c) the super mode spectra of the generated 10-GHz optical pulses when a 1-m unpumped EDF with an absorption coefficient of 13 dB/m @ 1530 nm is incorporated, and the optical powers in the counterclockwise and clockwise directions are 15.6 and 2 dBm, respectively.

suppression ratio in the OEO loop. In addition, the phase noise of the system can be further improved by optimizing the system parameters, such as the dispersion of the fiber laser loop, and the lengths of the fiber laser and the OEO cavity.

The stability of the proposed COEO in the laboratory environment is also investigated. With the proposed strong standing-wave forming structure, no significant spectral fluctuation and time drift is found in a 1.5-hour observation. The optical components in the cavity, including the EDF used in the strong standing wave forming structure, are not polarization maintained. If the optical components used in the system are polarization-maintained, the performance and the stability of the proposed COEO can be further improved. In addition, the system can be packaged to reduce the environmental influence. Feedback-controlling circuits can also be used to control the parameters of the system, such as the bias voltage, the EDFA gain, the temperature and so on, to make the COEO more stable.

B. Investigation of the Influence of the Unpumped EDF's Key Parameters

The system performance is affected by the incorporated unpumped EDF's length and the doping concentration (represented by the absorption coefficient here). Firstly, the effect of the

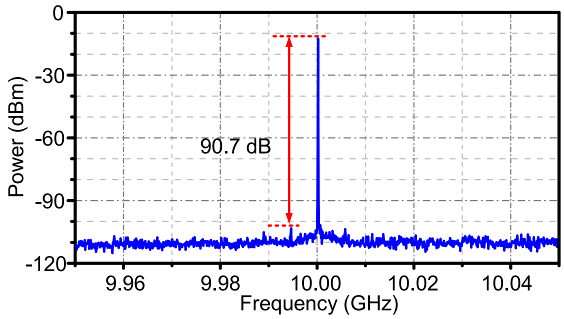

(a)

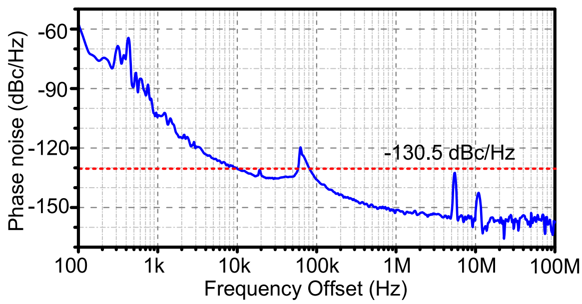

(b)

Fig. 5. (a) The electrical spectrum and (b) the phase noise of the generated 10-GHz microwave signal when a 1-m unpumped EDF with an absorption coefficient of 13 dB/m @ 1530 nm is incorporated, and the optical powers in the counterclockwise and clockwise directions are 15.6 and 2 dBm, respectively.

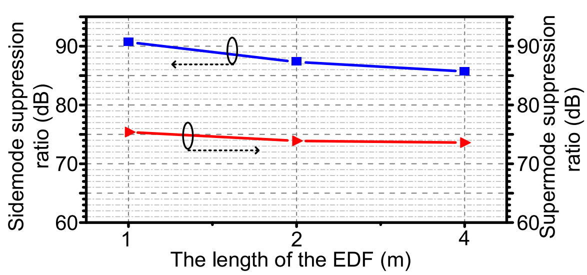

Fig. 6. Sidemode suppression ratio and supermode suppression ratio versus the length of the EDF when an unpumped EDF with an absorption coefficient of 13 dB/m @ 1530 nm is incorporated, and the optical power in the counterclockwise and clockwise directions are 15.6 and 2 dBm, respectively.

EDF's length is investigated by incorporating 1-, 2- and 4-m unpumped EDF with an absorption coefficient of 13 dB/m @1530 nm in the strong standing-wave forming structure, respectively. The optical powers in the clockwise and counterclockwise direction are kept to be 2 and 15.6 dBm, respectively. The sidemode suppression ratio and the supermode suppression ratio values versus the length of the EDF are shown in Fig. 6. It can be seen that when the length of the EDF with an absorption coefficient of 13 dB/m @ 1530 nm is 1 m, the optimized sidemode suppression ratio of 90.7 dB and supermode suppression ratio of 75.4 dB can be achieved. With the increasing of the EDF's length, for the 2- and 4-m EDF conditions, the sidemode suppression ratio is decreased to 87.3 and 85.7 dB, respectively, and supermode suppression ratio also decreases to be 73.9 and 73.6 dB, respectively. Thus an optimized length of the unpumped EDF exists. This is because on one hand, the length of the EDF should be

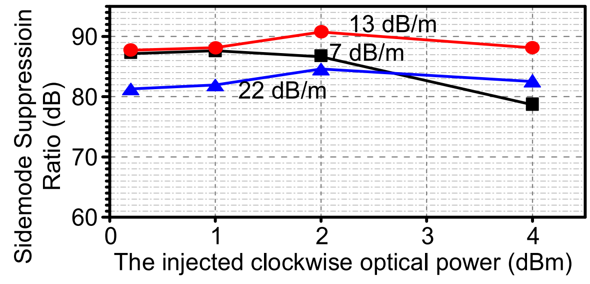

(a)

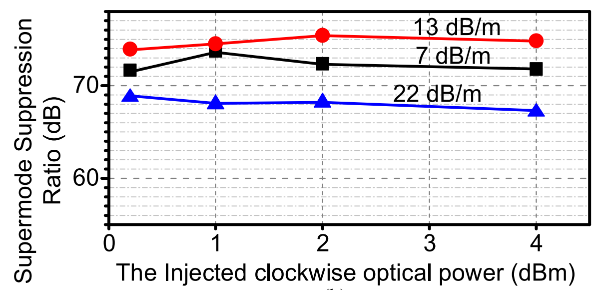

(b)

Fig. 7. (a) The sidemode suppression ratio and (b) the supermode suppression ratio versus the injected clockwise optical power when 1-m unpumped EDF with an absorption coefficient of 7, 13 and 22 dB/m @ 1530 nm is incorporated, and the optical power in the counterclockwise direction is 15.6 dBm.

long enough to form the required SHB effect to suppress the undesired supermodes. From Eqs. (2) and (3), it can be seen that the FWHM bandwidth of the self-induced FBG decreases with the increase of the EDF's length, which will improve the supermode suppression ratio. Meanwhile, the increasing of the EDF's length makes the length of the mode-locked fiber laser loop longer, and the mode spacing will be shortened, which may have an adverse effect on the supermode suppression performance.

Then the effect of the doping concentration of Er^{3+} is also investigated by incorporating unpumped EDFs with absorption coefficients of 7, 13 and 22 dB/m @ 1530 nm in the strong standing-wave forming structure, respectively. The lengths of the unpumped EDFs are fixed at 1 m. The optical power in the counterclockwise direction of the strong standing-wave forming structure is kept to be 15.6 dBm. Fig. 7(a) shows the sidemode suppression ratio of the generated RF signal in the OEO loop versus the injected clockwise optical power, and the supermode suppression ratio performance of the generated optical pulse is shown in Fig. 7(b). It can be seen that the by using absorption coefficient of 13 dB/m @ 1530 nm for the 1-m unpumped EDF condition, the sidemode suppression and the supermode suppression performances are better than the 7- and 22- dB/m absorption coefficient conditions. It can be seen that for a fixed length of the unpumped EDF, the absorption coefficient has an optimized value. In addition, when the clockwise injected optical power is increased to be larger than 4 dBm, the stability of the COEO will be deteriorated. According to Eq. (3), the filtering performance of the self-induced FBG is related to the induced maximum refraction index change Δn, which is proportional with the doping concentration as well as the absorption coefficient. A proper

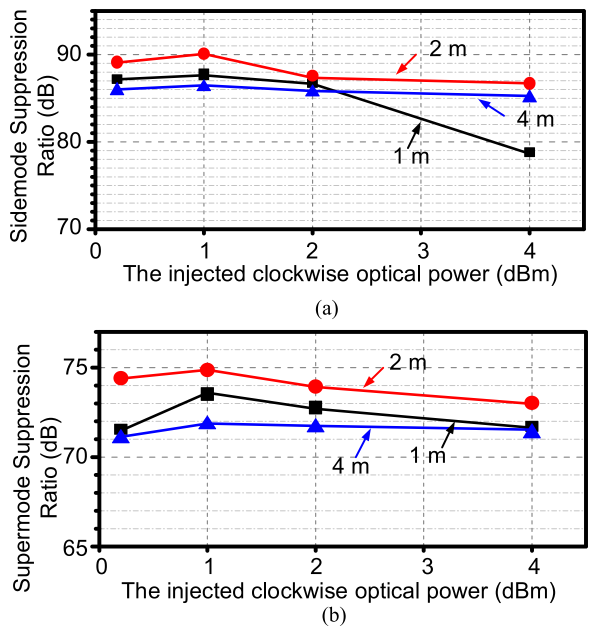

Fig. 8. (a) The sidemode and (b) the supermode suppression ratio versus the injected clockwise optical power when 1-, 2- and 4-m unpumped EDF with an absorption coefficient of 7 dB/m @ 1530 nm is incorporated, and the counterclockwise optical power is 15.6 dBm.

absorption coefficient should be provided to guarantee the forming of the absorption effect. On the other hand, the absorption coefficient should not be too large, for which condition the FWHM bandwidth of the self-induced FBG filtering characteristic will be too large and the supermode suppression performance will be affected.

The effects of the EDF's length and the injected clockwise optical power (corresponding to the strength of the forming standing wave) for different absorption coefficient conditions are also investigated. Changing the absorption coefficient of the unpumped EDF to be 7 dB/m @ 1530 nm, Fig. 8(a) shows the sidemode suppression ratio of the generated RF signal in the OEO loop versus the injected clockwise optical power by incorporating a 1-, 2- and 4-m unpumped EDF, respectively, while the corresponding supermode suppression performance is shown in Fig. 8(b). The optical power in the counterclockwise direction of the strong standing-wave forming structure is kept to be 15.6 dBm. It can be seen that by using a 2-m EDF for the absorption coefficient of 7 dB/m @ 1530 nm condition, the sidemode suppression ratio and the supermode suppression ratio performances are better than the 1- and 4-m EDF conditions. As compared to the condition with the absorption coefficient of 13-dB/m @ 1530 nm, the optimized length of the EDF is increased to be 2 m due to the decreasing of the absorption coefficient. In addition, an optimized clockwise optical power of 1 dBm exists, with 74.9-dB supermode suppression ratio and 90.1-dB supermode suppression. The corresponding phase noise of the generated microwave signal is measured to be -130.2 dBc/Hz at 10-kHz offset. It also can be seen that most of the supermode and sidemode suppression performances are correlated. It is because the supermodes and sidemodes share the same origin in COEO at the steady state. When the injected clockwise optical power is 4 dBm, a drop can be observed for the sidemode suppression ratio performance for the condition incorporating 1-m EDF with 7-dB/m @1530 nm absorption coefficient, as shown in Figs. 7(a) and 8(a). This is because the steady working state of the COEO is destroyed at this point. With the clockwise optical power increased to 4 dBm, the unpumped EDF cannot absorb all the optical power, and the residual power will leak into the EDFA and make the system unstable.

The set of the optimized key parameters for the 22-dB/m @ 1530 nm absorption coefficient condition are also investigated in the same way. The optimized length of the EDF is measured to be 1 m. An optimized clockwise optical power of 2 dBm exists, with the supermode suppression ratio to be 68.2 dB and the supermode suppression to be 84.6 dB. The corresponding phase noise of the generated microwave signal is shown to be -125.9 dBc/Hz at 10-kHz offset. It can be seen that the optimized performance of the COEO with the 13-dB/m @ 1530 nm absorption coefficient condition is better than the 7- and 22-dB/m @1530 nm absorption coefficient conditions. This is because with a proper absorption coefficient, a suitable injection power (neither too large nor too small) is used to avoid the nonlinearities and the length of the EDF also has a suitable value to avoid the negative effect of increasing the length of the cavity.

IV. Discussions and Conclusions

A COEO incorporating a strong standing-wave forming structure to introduce enhanced SHB effect in an unpumped EDF is proposed and demonstrated. A novel enhanced standing-wave forming structure is introduced to form strong standing waves in the unpumped EDF, which enables large SHB effect to improve the performance of the system. A 10-GHz COEO is experimentally established. A 10-GHz stable optical pulse train is generated with 75.4-dB supermode suppression ratio. Meanwhile, a 10-GHz RF signal with high quality is generated with 90.7-dB sidemode suppression ratio and phase noise of -130.52 dBc/Hz at 10-kHz offset. As compared with the results in [24], significant improvement is achieved by optimizing the parameters of the system, including a 7-dB improvement of the phase noise (from -123.6 to -130.52 dBc/Hz at 10-kHz offset) and a 15-dB improvement of the sidemode suppression ratio measured at the RF output of the OEO loop (from about 74.7 dB to 90.0 dB).

The proposed scheme can support multi-wavelength operation when the wavelength spacing is much larger than the two nearest longitudinal modes' spacing. In addition, the tunability of the COEO can also be realized if the fixed bandpass filter in the OEO loop is replaced by a tunable filter. The simplicity of the scheme is guaranteed since the strong standing wave is formed through a simple structure, and neither long fiber nor multi-loop structure is required. The system performances in both optical and microwave domains are significantly improved. The proposed scheme can find applications in high-speed photonic signal generation and processing systems.

REFERENCES

[1] X. S. Yao and L. Maleki, "Dual microwave and optical oscillator," *Opt. Lett.*, vol. 22, no. 24, pp. 1867–1869, Dec. 1997.

[2] X. S. Yao, L. Davis, and L. Maleki, "Coupled optoelectronic oscillators for generating both RF signal and optical pulses," *J. Lightw. Technol.*, vol. 18, no. 1, pp. 73–78, Jan. 2000.

[3] B. Matsko, D. Eliyahu, and L. Maleki, "Theory of coupled optoelectronic microwave oscillator II: Phase noise," *J. Opt. Soc. Amer. B.*, vol. 30, no. 12, pp. 3316–3323, Dec. 2013.

[4] W. Loh *et al.*, "Low-noise RF-amplifier-free slab-coupled optical waveguide coupled optoelectronic oscillators: Physics and operation," *Opt. Express*, vol. 20, no. 17, pp. 19420–19430, Aug. 2012.

[5] O. Lelievre *et al.*, "Experimental design of a low phase noise coupled optoelectronic oscillator at 10 GHz," in *Proc. Int. Top. Meet. Microw. Photon.*, Beijing, China, Oct. 23–26, 2017, pp. 1–4.

[6] P. Ghelfi *et al.*, "A fully photonics-based coherent radar system," *Nature*, vol. 507, pp. 341–345, Mar. 2014.

[7] S. L. Pan *et al.*, "Satellite payloads pay off," *IEEE Microw. Mag.*, vol. 16, no. 8, pp. 61–73, Sep. 2015.

[8] J. S. Wey, J. Goldhar, and G. L. Burdge, "Active harmonic modelocking of an erbium fiber laser with intracavity Fabry-Perot filters," *J. Lightw. Technol.*, vol. 15, no. 7, pp. 1171–1180, Jul. 1997.

[9] N. Onodera, "Supermode beat suppression in harmonically mode-locked erbium-doped fiber ring lasers with composite cavity structure," *Electron. Lett.*, vol. 33, no. 11, pp. 962–963, May 1997.

[10] S. L. Pan, C. Y. Lou, and Y. Z. Gao, "Multiwavelength erbium-doped fiber laser based on inhomogeneous loss mechanism by use of a highly nonlinear fiber and a Fabry-Perot filter," *Opt. Express*, vol. 14, no. 3, pp. 1113–1118, Feb. 2006.

[11] M. Nakazawa, K. Tamura, and E. Yoshida, "Supermode noise suppression in a harmonically mode-locked fiber laser by self-phase modulation and spectral filtering," *Electron. Lett.*, vol. 32, no. 5, pp. 461–463, Feb. 1996.

[12] C. R. Doerr, H. A. Haus, E. P. Ippen, M. Shirasaki, and K. Tamura, "Additive-pulse limiting," *Opt. Lett.*, vol. 19, no. 1, pp. 31–33, Jan. 1994.

[13] Y. Dai *et al.*, "Sidemode suppression for coupled optoelectronic oscillator by optical pulse power feedforward," *Opt. Express*, vol. 23, no. 21, pp. 27589–27596, Oct. 2015.

[14] F. Quinlan, S. Gee, S. Ozharar, and P. J. Delfyett, "Greater than 20-dB supermode noise suppression and timing jitter reduction via CW injection of a harmonically mode-locked laser," *IEEE Photon. Technol. Lett.*, vol. 19, no. 16, pp. 1221–1223, Jul. 2007.

[15] C. M. Wu and N. K. Dutta, "High-repetition-rate optical pulse generation using a rational harmonic mode-locked fiber laser," *IEEE J. Quantum Electron.*, vol. 36, no. 2, pp. 145–150, Feb. 2000.

[16] T. Hirooka, K. Tokuhhira, M. Yoshida, and M. Nakazawa, "440 fs, 9.2 GHz regeneratively mode-locked erbium fiber laser with a combination of higher-order solitons and a SESAM saturable absorber," *Opt. Express*, vol. 24, no. 21, pp. 24255–24264, Oct. 2016.

[17] D. Zhu, T. H. Du, and S. L. Pan, "A coupled optoelectronic oscillator based on a resonant saturable absorber mirror," presented at the 32nd URSI Gen. Assem. Sci. Symp., Montreal, QC, Canada, Aug. 19–26, 2017.

[18] E. Salik, N. Yu, and L. Maleki, "An ultralow phase noise coupled optoelectronic oscillator," *IEEE Photon. Technol. Lett.*, vol. 19, no. 6, pp. 444–446, Mar. 2007.

[19] N. Yu, E. Salik, and L. Maleki, "Ultralow-noise mode-locked laser with coupled optoelectronic oscillator configuration," *Opt. Lett.*, vol. 30, no. 10, pp. 1231–1233, May 2005.

[20] X. S. Yao and L. Maleki, "Multiloop optoelectronic oscillator," *IEEE J. Quantum Electron.*, vol. 36, no. 1, pp. 79–84, Jan. 2000.

[21] S. H. Cai, S. L. Pan, D. Zhu, and X. F. Chen, "Stabilize the coupled optoelectronic oscillator by an unpumped erbium-doped fiber," presented at the Asia Commun. Photon. Conf., Guangzhou, China, 2012, Paper ATh2C.5.

[22] M. Jiang, X. Q. Dinh, P. P. Shum, S. Molin, Z. F. Wu, and P. Nouchi, "Investigation of axial strain effects on microwave signals from a PM-EDF short cavity DBR laser for sensing applications," *IEEE Photon. J.*, vol. 4, no. 5, pp. 1530–1535, Aug. 2012.

[23] Z. W. Wei, D. Zhu, and S. L. Pan, "Stabilize the regeneratively mode-locked fiber laser based on a polarization maintained dual-loop structure," presented at the Asia Commun. Photon. Conf., Hong Kong, China, 2015, Paper ASu5I. 1.

[24] D. Zhu, Z. W. Wei, T. H. Du, and S. L. Pan, "A coupled optoelectronic oscillator based on enhanced spatial hole burning effect," in *Proc. Avionics Veh. Fiber-Opt. Photon. Conf. Int. Top. Meet. Microw. Photon.*, Long Beach, CA, USA, Oct. 31-Nov. 3, 2016, pp. 177–180.

[25] S. Zhao, P. Lu, L. Chen, D. Liu, and J. Zhang, "Transient bragg fiber gratings formed by unpumped thulium doped fiber," *Front. Optoelectron.*, vol. 6, no. 2, pp. 180–184, Jun. 2013.

[26] E. Desurvire, "Study of the complex atomic susceptibility of erbium doped fiber amplifiers," *J. Lightw. Technol.*, vol. 8, no. 10, pp. 1517–1527, Oct. 1990.

[27] 2017. [Online]. Available: http://www.yofc.com/wcs/Upload/201704/58ef29e305f66.pdf

[28] J. L. Wagener, P. F. Wysocki, M. J. Digonnet, H. J. Shaw, and D. J. Digiovanni, "Effects of concentration and clusters in erbium-doped fiber lasers," *Opt. Lett.*, vol. 18, p. 2014, Dec.1993.

Dan Zhu (M'12) received the B.S. and Ph.D. degrees in electronics engineering from Tsinghua University, Beijing, China, in 2004 and 2009, respectively.

In July 2009, she joined the Research Department of Radar Signal Processing, China Electronics Technology Group Corporation No. 14 Research Institute, as a Researcher. In May 2011, she joined the Key Laboratory of Radar Imaging and Microwave Photonics, Ministry of Education, Nanjing University of Aeronautics and Astronautics, Nanjing, China, where she is currently an Associate Professor. Her current research interests include photonic microwave and millimeter wave generation and optical signal processing.

Dr. Zhu is a member of the IEEE Microwave Theory and Techniques Society, the IEEE Photonics Society, and the Optical Society of America.

Tianhua Du, biography not available at the time of publication.

Shilong Pan (S'06–M'09–SM'13) received the B.S. and Ph.D. degrees in electronics engineering from Tsinghua University, Beijing, China, in 2004 and 2008, respectively.

From 2008 to 2010, he was a "Vision 2010" Postdoctoral Research Fellow with the Microwave Photonics Research Laboratory, University of Ottawa, Canada. He joined the College of Electronic and Information Engineering, Nanjing University of Aeronautics and Astronautics, Nanjing, China, in 2010, where he is currently a Full Professor and an Executive Director of the Key Laboratory of Radar Imaging and Microwave Photonics, Ministry of Education. He has authored or co-authored more than 360 research papers (citations: more than 3400, H-index: 31), including more than 190 papers in peer-reviewed journals and 170 papers in conference proceedings. His research focuses on microwave photonics, which include optical generation and processing of microwave signals, analog photonic links, photonic microwave measurement, and integrated microwave photonics.

Prof. Pan is currently a Topical Editor for the *Chinese Optics Letters*, and is a Technical Committee Member of the IEEE MTT-3 Microwave Photonics. He is a Steering Committee Member of the IEEE International Topical Meeting on Microwave Photonics and International Conference on Optical Communications and Networks. He has also served as a Chair of a number of international conferences, symposia, and workshops, including the TPC Chair of the International Conference on Optical Communications and Networks in 2015, the TPC Co-Chair of the *IEEE International Topical Meeting on Microwave Photonics* in 2017, the TPC Chair of the high-speed and broadband wireless technologies subcommittee of the *IEEE Radio Wireless Symposium* in 2013, 2014, and 2016, respectively, the TPC subcommittee Chair of the OptoElectronics and Communication Conference in 2015, the TPC subcommittee Co-Chair of the CLEO Pacific Rim in 2018, the International Conference on Information Optics and Photonics in 2018, and the Chair of the microwave photonics for broadband measurement workshop of the International Microwave Symposium in 2015.

Prof. Pan is a Senior Member of the IEEE Microwave Theory and Techniques Society, the IEEE Photonics Society, and a Senior Member of the Optical Society of America. He was selected to receive an OSA outstanding reviewer award in 2015 and a top reviewer of the IEEE/OSA JOURNAL OF LIGHTWAVE TECHNOLOGY in 2016. He received the Excellent Young Scholars Award of the National Natural Science Foundation of China in 2014, and the Scientific and Technological Innovation Leading Talents Award of the National Ten Thousand Plan in 2018.